Periodic precipitation patterns in the presence of concentration gradients. 2. Spatial bifurcation of precipitation bands and stochastic pattern formation

ARTICLE *in* THE JOURNAL OF PHYSICAL CHEMISTRY · MARCH 1983

Impact Factor: 2.78 · DOI: 10.1021/j100228a022

3 AUTHORS:

Shoichi Kai
Kyushu University
228 PUBLICATIONS **2,555** CITATIONS
SEE PROFILE

Stefan C Müller
Otto-von-Guericke-Universität Magdeburg
288 PUBLICATIONS **5,065** CITATIONS
SEE PROFILE

John Ross
Stanford University
89 PUBLICATIONS **2,625** CITATIONS
SEE PROFILE

Periodic Precipitation Patterns in the Presence of Concentration Gradients. 2. Spatial Bifurcation of Precipitation Bands and Stochastic Pattern Formation

Shoichi Kai,† Stefan C. Müller,‡ and John Ross*

Department of Chemistry, Stanford University, Stanford, California 94305 *(Received: July 9, 1982)*

We report on two phenomena observed in periodic precipitation patterns (Liesegang rings) of lead iodide which evolve during the interdiffusion of lead nitrate and potassium iodide, such that the initial difference Δ between the two electrolyte concentrations or the initial ion product σ of the electrolytes are small: (1) A spatial bifurcation occurs of a single sharp band into two clearly separated sharp bands of precipitate as Δ is increased from zero to a nonzero but small value while σ is kept constant; both bands are located within a broad zone of low-density colloid of lead iodide. The bifurcation is studied by visual observations and by measurements of the intensity of transmitted light. (2) The precipitation patterns are found to be increasingly stochastic, in terms of probability of ring formation and the reproducibility of the location of rings, as either the value of Δ is decreased to zero or the value of σ approaches a lower limit, below which no structure is observed. The experiments on the distribution of ring locations are represented by histograms to which in most, but not all, cases a Gaussian distribution function can be fitted. We also report results on several types of precipitation patterns of lead iodide obtained in the absence of any imposed macroscopic gradients of electrolyte concentrations. The experiments show the continuous progression of structure formation, from high to zero initial concentration gradients, and thus lead to the suggestion that the origin of pattern formation is the same in all cases.

I. Introduction

In this article we continue our study of perodic precipitation patterns (Liesegang rings[1-3]) in the presence of concentration gradients. See the following references for the background and motivation,[4,5] prior experiments,[3-10] and theories.[6,7,11-15] In part I, ref 5, we reported a series of experiments in which we measured the number of precipitation bands (rings) formed, the ring spacing, and the ring width for wide ranges of initial concentrations of electrolytes. We showed that the initial concentration difference, $\Delta = 1/2[I^-] - [Pb^{2+}]$, for PbI_2 for instance, and the initial ion product, $\sigma = [Pb^{2+}][I^-]^2$, are useful parameters to characterize the variability of precipitation patterns. A simple ring spacing law is obtained only when σ and Δ are large. No band formation occurs below a critical value of σ. As σ and Δ are lowered, the bands broaden, and their location varies in a complex manner. For low values of σ and Δ, zones of colloid evolve prior to the appearance of one or two bands within such zones.

We report here observations and measurements of two phenomena occurring in Liesegang systems with very low initial values of Δ or σ (and corresponding low concentration gradients), which we believe to be important for a better understanding of the processes involved in the ring formation mechanism. These are the following: (1) the spatial separation of one band into two precipitation bands, both located within a broad zone of colloidal material, as the concentration difference Δ is increased from zero to small values, while σ is maintained constant (spatial "bifurcation"); (2) a pronounced increase of the randomness in the appearance and the location of bands when either Δ or σ is decreased to values close to zero. No reference to these phenomena is made in the literature and we have found no prior detailed work on the formation of precipitation patterns with very low imposed gradients. We also include a brief description of several types of patterns which arise from initially homogeneous salt solutions.[6-8] The experiments are designed to show the connection, if any, between structure formation in systems with and without initial concentration gradients.

All our experiments were performed with lead iodide as the precipitating salt. Section II gives preparation procedures and concentration specifications for several series of experiments. The results are presented in three parts: an illustration of the bifurcation phenomenon and its relationship to the extent and the density of the zones of colloidal material in which the bifurcated bands are embedded (section IIIA); a qualitative description and an evaluation by statistical methods of the stochastic features in the formation and the location of rings for low initial values of σ and vanishing Δ (section III.B); and a short presentation of some structural features of inhomogeneous precipitation patterns formed in the absence of any macroscopic gradients (section III.C).

II. Experiments

A. Preparations. The reagents used for Liesegang ring formation of PbI_2 were solutions of low concentration of $Pb(NO_3)_2$ (1.7–17 mM) and KI (14–70 mM), both containing 1% agar-agar gel. Our procedure for preparing

† Present address: Department of Electronics, Kyushu University, Fukuoka 812, Japan.

‡ Present address: Max-Planck-Institut für Ernährungsphysiologie, D-4600, Dortmund, West Germany.

(1) R. E. Liesegang, *Naturwiss. Wochenschr.* 11, 353 (1896).
(2) E. S. Hedges, "Liesegang Rings and Other Periodic Structures", Chapman and Hall, London, 1932.
(3) K. H. Stern, *Chem. Rev.*, **54**, 79 (1954); "A Bibliography of Liesegang Rings", 2nd ed., U.S. Government Printing Office, Washington, DC, 1967.
(4) S. Kai, S. C. Müller, and J. Ross, *J. Chem. Phys.*, **76**, 1392 (1982).
(5) S. C. Müller, S. Kai, and J. Ross, *J. Phys. Chem.*, **86**, 4078 (1982).
(6) M. Flicker and J. Ross, *J. Chem. Phys.*, **60**, 3458 (1976).
(7) D. Feinn, P. Ortoleva, W. Scalf, S. Schmidt, and M. Wolff, *J. Chem. Phys.*, **69**, 27 (1978).
(8) S. C. Müller, S. Kai, and J. Ross, *Science*, **216**, (1982).
(9) S. C. Müller, S. Kai, and J. Ross, *J. Phys. Chem.*, submitted.
(10) F. D. Gnanam, S. Krishnan, P. Ramasamy, and G. S. Laddha, *J. Colloid Interface Sci.*, **73**, 193 (1980).
(11) W. Ostwald, "Lehrbuch der Allgemeinen Chemie", Engelman, Leipzig, 1897.
(12) S. Prager, *J. Chem. Phys.*, **25**, 279 (1956).
(13) J. B. Keller and S. I. Rubinow, *J. Chem. Phys.*, **74**, 5000 (1981).
(14) R. Lovett, P. Ortoleva, and J. Ross, *J. Chem. Phys.*, **69**, 947 (1978).
(15) G. Venzl and J. Ross, *J. Chem. Phys.*, **77**, 1302, 1308 (1982).

0022-3654/83/2087-0806$01.50/0

TABLE I: Initial Values of the Concentration Difference $\Delta = {}^1/_2[I^-] - [Pb^+]$, the Ion Product $\sigma = [Pb^+][I^-]^2$, $S = \sigma/\sigma_0$ ($\sigma_0 = 1.39 \times 10^{-8}$ M^3), and Number of Tubes M_{tot} for Each Combination of Δ and σ in Groups A and B of the Experiments

A-1	0.0, 0.9, 1.8, 2.6, 4.2, 5.6, 7.1, 8.4, 10.8, 12.1, 14.0, 16.1, 18.2, 20.0, 22.6, 25.0	1.8	1300	
A-2	0.0, 1.2, 2.7, 5.1, 7.5, 9.0, 14.6, 16.0, 18.1, 19.9, 24.1	1.4	1007	3
A-3	0.0, 0.9, 1.6, 2.5, 4.0, 5.4, 6.7, 8.0, 9.1, 10.7, 11.7, 15.5, 19.2	0.7	504	
B-1	13.6	2.1	1510	30
		1.3	935	21
		0.91	655	26
B-2	10.8	1.8	1300	10
	2.4			15
	0.9			15
	0.0			30
B-3	0.0	1.4	1007	35

Liesegang experiments has been described elsewhere.[5] The tubes (inner diameter, 5.3 mm) were always kept in a horizontal position until completion of the pattern formation after 3 to up to 30 days; we thus excluded any effects due to the gravitational field.[4,5] The amount of each gel solution in each tube was 1 mL. For all investigated systems the initial concentration difference $\Delta = 1/2[I^-] - [Pb^{2+}]$ was positive or zero; that is, PbI_2 precipitation bands appeared in the lead solution.[5]

For the purpose of performing experiments without imposed gradients of concentration a small amount of PbI_2 (4–6.5 mM) was dissolved in water at 95 °C (solubility at 95 °C: 8.7 mM[16]) and 0.2–1.0 % agar-agar gel was added. The hot solutions were thoroughly mixed for 20 min until homogeneous. At a temperature of 80 °C they were poured into glass containers of different geometries, preheated to the same temperature. Preferentially flat containers such as Petri dishes (diameter, 20–140 mm) were used; their bottom was covered by layer of 1–2-mm thickness of the solution. The hot containers were placed on an insulting material, covered, and allowed to cool at room temperature or at 0 °C. After approximately 1 h the gel had solidified, and within the next few hours spatially inhomogeneous patterns of yellow precipitate of PbI_2 became visible to the eye, provided that the concentrations of the gel and the salt had been chosen properly. The containers were left undisturbed for at least 2 days. After this time no further changes occurred in the precipitation patterns.

B. Concentration Specifications and Measurements. Our experiments on Liesegang rings are arranged in two groups, A and B, each consisting of several series of tubes with varying initial conditions of the concentration difference Δ, the ion product σ, and the number of tubes M_{tot} prepared for each of the combinations of Δ and σ. The values of Δ, σ, and $S = \sigma/\sigma_0$, where σ_0 denotes the solubility product of PbI_2 in water ($\sigma_0 = 1.39 \times 10^{-8}$ M^3 at 25 °C[16]), for the three series A-1–A-3 of this group are listed in Table I.[17] In order to check roughly the reproducibility of the patterns in group A, we usually chose $M_{tot} = 3$ (see also Section II.C in ref 5). In the second group we focused on the problem of pattern reproducibility. For several values of Δ and σ we simultaneously prepared a number of tubes (10–35) of the same geometry with identical electrolyte solutions of equal volumetric amounts. The lower the reproducibility of the patterns, the larger number of identical tubes chosen. Specifications of Δ, σ, S, and M_{tot} for the three series B-1–B-3 of this group are given in Table I.

We followed the temporal evolution of the Liesegang systems by visual observation and by measurements of the location of those structural features which are clearly defined, such as the location and width of rings and the extent of zones of low-density colloid (detectable by the distinct yellow color of PbI_2, see section III.A). We also took negatives of the patterns at regular time intervals; we scanned each of the negatives of the tubes along its vertical axis with a focused laser beam and recorded the intensity of transmitted light I_t as a function of the space coordinate x. The spatial resolution of this procedure, which provides qualitative results on colloid densities, is sufficient to resolve structural features on a length scale of 0.2 mm.

Visual observations are reported on structure formation in precipitating systems without imposed concentration gradients.

III. Results

A. Spatial Bifurcation with Variation of Concentration Difference. The temporal development of the precipitation patterns in the tubes of series A-1 with $\Delta > 2$ mM ($\sigma = 1.8 \times 10^{-5}$ M^3) is shown in Figure 1: after 2 days (A), 6 days (C), and 1 month (D). Increasing tube number indicates increasing concentration difference Δ, as specified in the caption. In figure 1A,C tubes 2 and 3 are omitted; Figure 1D represents the final pattern of the entire set of tubes. The graphs of Figure 1B are plots of the intensity of transmitted light I_t vs. the space coordinate x for each of the tubes of Figure 1A, obtained as described in the previous section. Their purpose is to show all the qualitative features of the patterns in terms of the translucency of the colloid or precipitate of PbI_2 formed.[16] The patterns do not simply consist of a set of well-focused bands of precipitate. This is only the case when both the values of Δ and σ are fairly high, while for low Δ or σ the precipitation bands tend to be surrounded by zones of low-density colloid, as has been pointed out previously.[5] The main features of the patterns after 2 days (Figure 1A,B) are the following: (1) Rings of high-density precipitate have formed in tubes 4–13 ($\Delta > 5$ mM). The location of their centers is indicated by the full triangles. Most are well developed ($I_t = 0$ in B) and sharply focused, but a few are not so well recognizable, especially the first ring in each of the tubes 9–11 ($I_t \approx 0$ in B). Only one ring appears in tubes 4–9 ($\Delta \leq 16$ mM); its width increases slightly with increasing Δ and in tube 9 it is essentially a zone of colloid with low translucency (see graph 9 in Figure 1B). In each of the tubes 10–13 ($\Delta > 18$ mM) we observe two rings; the higher Δ, the more distinctively these two rings are separated from each other. By analogy to other phenomena we refer to the transition of one ring to two well-separated rings as a spatial bifurcation of a precipitation band. The concentration difference represents the pump parameter. The bifurcation point Δ_{bf} lies between tubes 9 and 10 ($16 < \Delta_{bf} < 18$ mM). (2) Zones of colloid of PbI_2 with varying translucency, corresponding to color variations from pale to deep yellow,[18] are visible in all tubes. (In systems with

(16) "Handbook of Chemistry and Physics, 60th ed., Chemical Rubber Publishing Co., Cleveland, OH, 1979.

(17) The same initial values for the concentration difference and the ion product were used in a series of investigations on the location of the first ring (ref 5).

(18) Variations in the color of the PbI_2 colloid correspond to only small variations in contrast in the photographs. Therefore, some details, which are observed visually, may not be recognizable in the photographs of Figures 1 and 4. The pictures in Figure 1, A and C, are slightly underexposed in order to render the faint zones of colloid clearly visible.

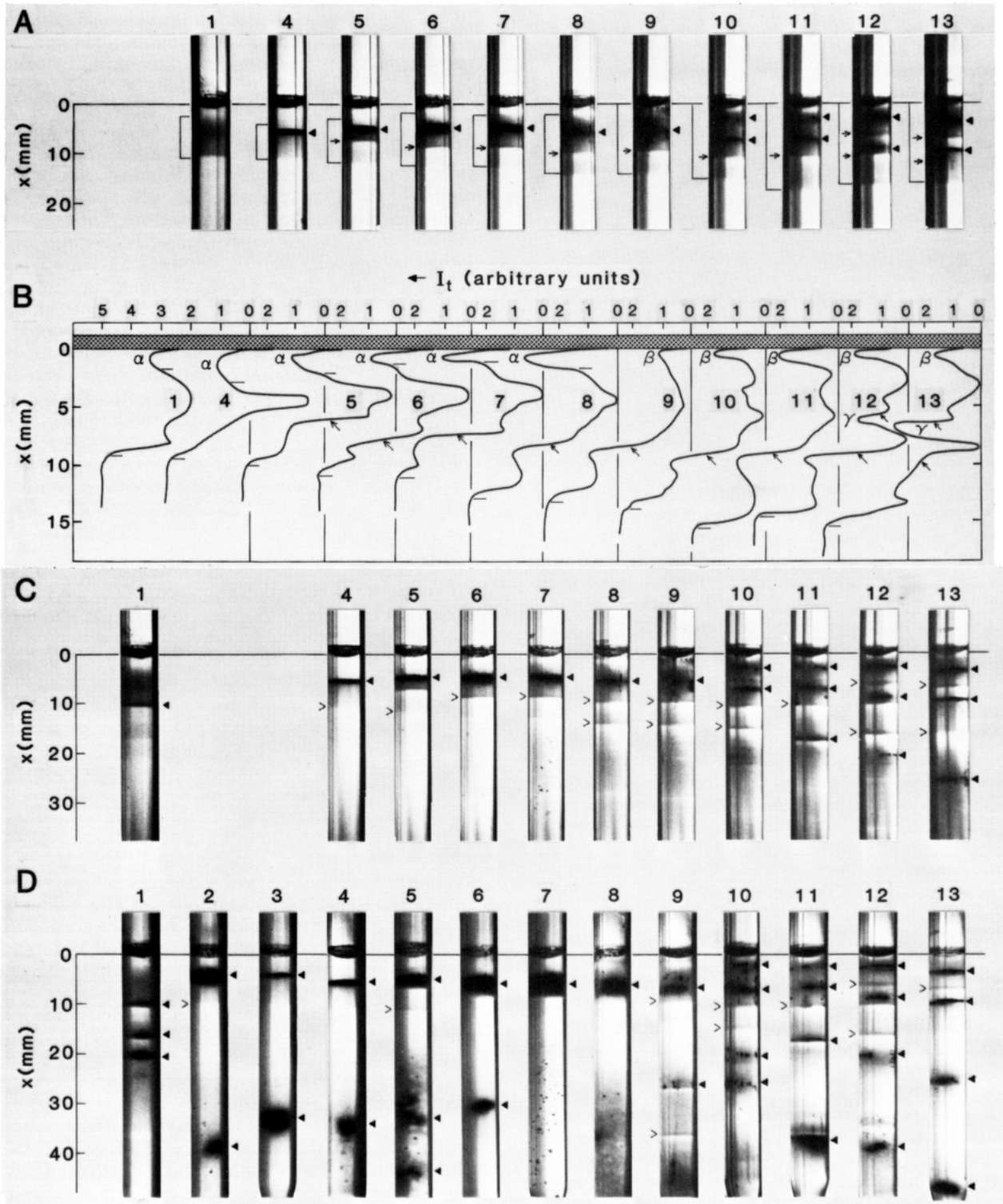

Figure 1. Precipitation patterns of tubes of series A-1 after 2 days (A), 6 days (C), and 1 month (D) with ion product $\sigma = 1.8 \times 10^{-5}$ M^3 and concentration difference $\Delta = 2.6, 4.2, 5.6, 7.1, 8.4, 10.8, 12.1, 14.0, 16.1, 18.2, 20.0, 22.6, 25.0$ mM for tubes 1–13, respectively. In graph B the intensity of light I_t transmitted through the negatives of each of the photographs of A is plotted as a function of the space variable x (see section II.B). The origin is shifted horizontally for each curve; the shaded area represents the precipitate at the initial junction between the electrolytes. The triangles point to the centers of Liesegang bands in A, C, and D; at the corresponding locations $I_t \approx 0$ in B. A spatial bifurcation of the first band into two well-separated bands occurs between tubes 9 and 10 ($16 < \Delta_{bf} < 18$ mM). The bands are surrounded by zones of low-density colloid of PbI_2; the angular brackets in A and the horizontal bars in B mark the extent of these zones after 2 days. The pointed angles in C and D indicate faint striations in the colloidal distribution which remain visible at later times. For further details see text.

$\Delta < 2$ mM, not shown in the figure, no colloid was visually detected after 2 days.) The extent of the zones is marked by angular brackets in Figure 1A and by horizontal bars in Figure 1B. They extend well beyond the ring location and their width smoothly increases with increasing Δ. Note the clear narrow regions in tubes 1–8 between the junction and the colloidal zone, which are colorless and correspond to the pronounced maxima in I_t labeled α. Right next to the junction of tubes 9–13 there are similar, relatively translucent gaps. These, however, contain a small amount of visible colloid, observed by its distinct yellow color (maxima in I_t labeled β). Gaps of comparable, relatively high translucency also exist between the two rings in tubes 12 and 13 (maxima in I_t labeled γ). (3)

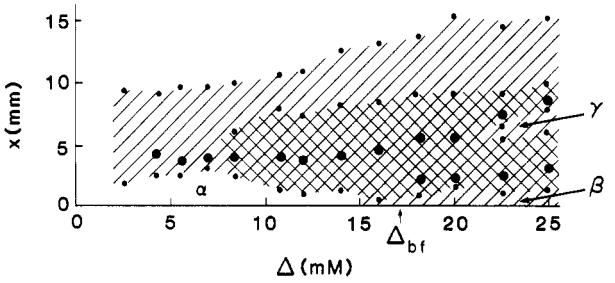

Figure 2. Sketch of zones of visible colloid and of locations of precipitation bands in series A-1 as a function of the concentration differences Δ, after 2 days, as derived from the transmission plots of Figure 1B. Two gradations of shading are used to distinguish between colloid of high and low translucency (light and dark shading, respectively). The small circles indicate the extent of the zones in each of the tubes 1–13 in Figure 1A,B. The locations of the centers of the precipitation bands are plotted as large circles. The bifurcation point Δ_{bf} is indicated. The letters α, β, and γ refer to the regions in which there are maxima in the I_t plots, labeled accordingly in Figure 1B.

There are additional structural features, the most remarkable of which is a steplike change in the density of the colloid (or its translucency) at a small distance in front of the last ring in all systems except for tubes 1–4 (arrows in Figure 1A,B). In tubes 12 and 13 with the highest Δ (>22 mM) such a step is observed twice, in front of each of the two rings.

The structural features just described are summarized by means of the rough sketch in Figure 2: On the basis of the I_t measurements of Figure 1B we plot the central location of the rings and the extent of zones of colloid as a function of Δ. We distinguish between colloid of low and intermediate translucency and represent these two qualitative categories by differently shaded areas. The increase of Δ gives rise to a "sequence" of structure formations (not to be confounded with a temporal sequence): formation of a zone of colloid; appearance of a ring at some location in this zone; broadening of the zone and formation of another, less extended zone of distinctively higher colloidal density on both sides of the ring; broadening of the ring and subsequent bifurcation into two separated rings; increase of the spacing between these rings and bifurcation of the denser zone of colloid. As a result we have two such zones, each of them associated with one of the two rings. Note that the location of the first ring x_1 decreases when Δ becomes larger than Δ_{bf}. This variation in x_1 has been described previously.[5]

After 6 days (Figure 1C) yellow colloid is visible all along the gel column of length of about 50 mm, not all of which is in the photographs of Figure 1C. On the average its density increases from left to right. Many, but not all of the steplike changes in colloid density, as observed after 2 days (Figure 1A,B), remain visible as faint striations in the spatial distribution of colloid and are marked by pointed angles. In a few cases, narrow bands of precipitate have developed at such locations, in particular at x = 10 mm in tube 1 and at x = 17 mm in tube 11, as marked by triangles. (The formation of the band in tube 1 is probably related to the small minimum at approximately the same location in the corresponding I_t plot of Figure 1B). Additional bands at larger values of x have formed in the systems with the highest values of Δ (tubes 12 and 13). Finally, after 1 month (Figure 1D), the total number of bands has grown to N = 4 in tubes 10–13, for which $\Delta > \Delta_{bf}$; an increase of Δ results, on the average, in an increase of the spacing between bands. Noticeably, for values of Δ slightly below Δ_{bf}, only one faint or no band has formed in addition to the first one (tube 9: N = 2; tubes 7, 8: N = 1), while the first band has grown substantially in width.

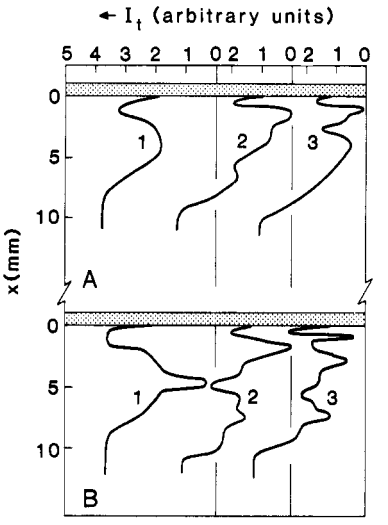

Figure 3. Early stages of precipitation patterns in three tubes of series A-2, after 16 (A) and 24 (B) h, with ion product $\sigma = 1.4 \times 10^{-5}$ M^3 and concentration difference Δ = 9.0, 18.1, 24.1 mM for tubes 1–3, respectively, represented by plots of the intensity of transmitted light I_t vs. x (compare Figure 1B and section II.A). Sharp minima of I_t correspond to bands of dense precipitate. After 16 h (A) there is one band in 2 and 3 at $x \approx 1.5$ mm and a second band has appeared in 3 at $x \approx 5$ mm which shows a bifurcation; after 24 h (B) there is one band in 1 at $x \approx 5$ mm, two bands in 2, and three bands in 3 indicating the onset of a spatial bifurcation between tubes 1 and 2 and another bifurcation between 2 and 3. Further details are described in the text.

TABLE II: Ion Product σ, the Bifurcation Value of the Concentration Difference Δ_{bf}, and the Quotient Δ_{bf}/σ for Group A of the Experiments

series	$10^5\sigma$, M^3	Δ_{bf}, mM	$\Delta_{bf}/(10^2\sigma)$ M^{-2}
A-1	1.8	16-18	8.9-10
A-2	1.4	10-15	7.2-10.7
A-3	0.7	6.8-8	9.7-11.4

In this range of Δ most of the colloidal material is incorporated in just one broad but well-defined spatial region and this structural feature is reproducibly found in system in which the bifurcation phenomenon occurs. With further decreasing Δ we again find at least one additional, broad band at comparatively large distances from the origin (tubes 1–6: N = 2 or 3). The lower the value of Δ, the more the locations of these bands are subject to statistical fluctuations, as discussed in section III.B. The patterns in tubes with Δ < 2 mM are included in that section.

The experiments of series A-2 and A-3 provide confirmation of the occurrence of a spatial bifurcation. In series A-2 with $12 < \Delta_{bf} < 15$ mM we focused on the very early stages of the precipitation process. In Figure 3 we present plots of the spatial variation of the transmitted light intensity I_t for the three values Δ = 9.0, 18.1, 24.1 mM. After 16 h (Figure 3A) two bands[19] have appeared in Figure 3A(3) which shows a bifurcation. After 24 h (Figure 3B) two bifurcations are visible: while only one band has appeared in 1 (I_t = 0 at x = 5 mm in system 1), an additional band begins to form for $\Delta > \Delta_{bf}$ (minimum in I_t at x = 8 mm in systems 2 and 3). In systems 3 with Δ = 24.1 mM we have three bands with the locations x_1 = 1.0 mm, x_2 = 2.5 mm, x_3 = 8 mm. Since the first two bands are at almost the same locations as the first band in system 2 (at x_1 = 1.5 mm), this observation suggests a second bifurca-

(19) The transmission plots in Figure 3A are comparable to those obtained during the temporal evolution of bands of $Mg(OH)_2$, as shown in Figure 6 of ref 4.

(20) The faint bands have been neglected in previous studies (ref 5).

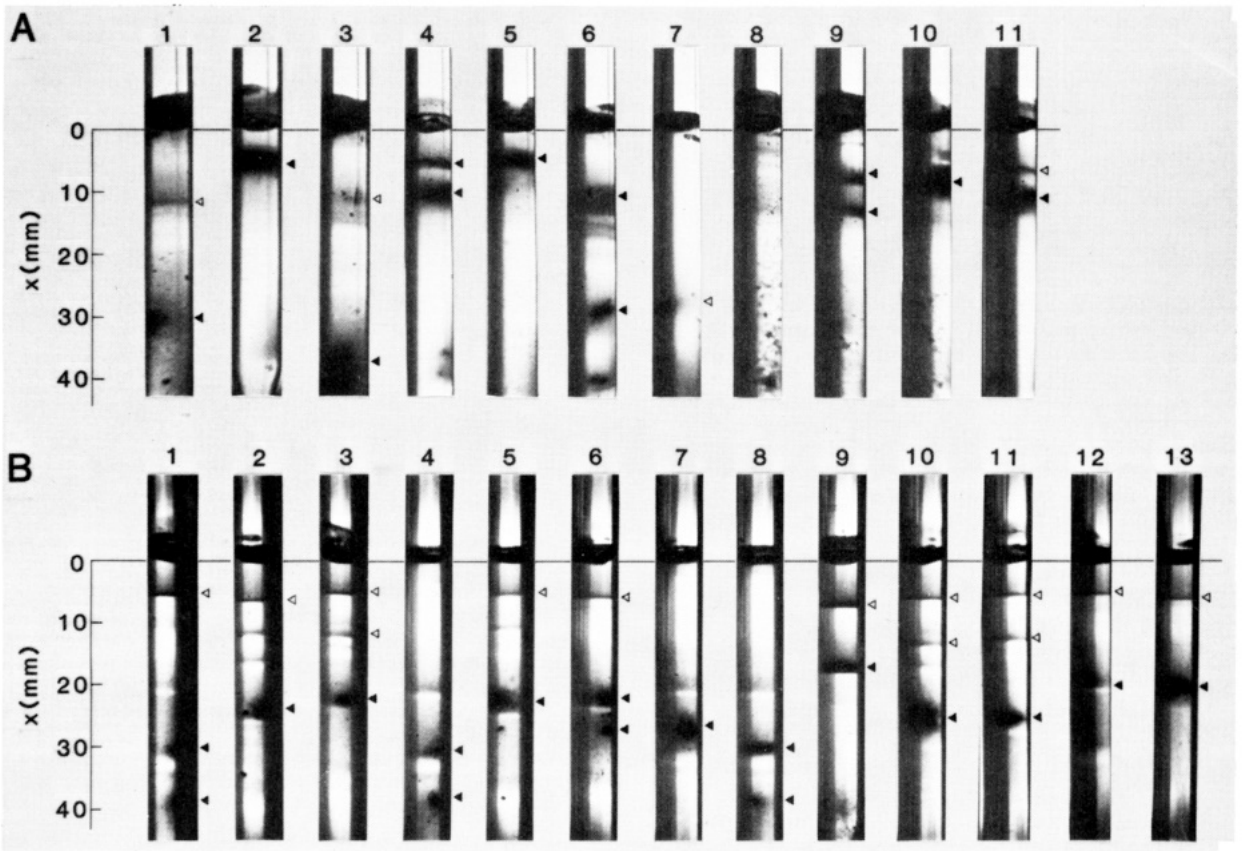

Figure 4. Liesegang band formation in two sets of tubes with identical initial electrolyte solutions, after 3 weeks. The experiment shows the stochastic element in the formation and the location of bands. Experimental conditions: (A) $\sigma = 1.4 \times 10^{-5}$ M^3, $\Delta = 0$, series B-3; (B) $\sigma = 1.8 \times 10^{-5}$ M^3, $\Delta = 0$, series B-2. Full and open triangles point to well-developed and faint bands, respectively.

tion of the first band in this series at a value of Δ slightly lower than 24 mM.

In Table II we list the estimated ranges of Δ_{bf} for each series of group A and the corresponding values for the quotient Δ_{bf}/σ which, in the rather small investigated range of σ, is approximately constant. More experiments with an extended range of σ are necessary to determine whether there is a linear relationship between Δ_{bf} and σ. Calculations show that the lead concentration is roughly the same as $\Delta = \Delta_{bf}$ in each of the three series (7.1 mM $\leq [Pb^{2+}]_{bf} \leq$ 8.4 mM); therefore, it is possible that this ion concentration plays a crucial role for the bifurcation phenomenon.

B. Stochastic Pattern Formation. The lack of reproducibility of Liesegang patterns which develop in systems with low initial values of Δ and σ has been pointed out in the previous section and in ref 5. In this section we use the results of group B of our experiments (see Table I) to study stochastic pattern properties at very low concentrations and concentration gradients.

1. Qualitative Description of Stochastic Patterns. In Figure 4 we show the final patterns after 3 weeks of two groups of initially identical sets of tubes selected from series B-3 (A: $\sigma = 1.4 \times 10^{-5}$ M^3, $\Delta = 0$) and from series B-2 (B: $\sigma = 1.8 \times 10^{-5}$ M^3, $\Delta = 0$). Some features to be noted are the following: (1) In almost all tubes of the figure we see at least one precipitation band which is clearly identifiable, even though mostly broad and diffuse (marked by full triangles); when there are two such bands, they tend to appear at closely adjacent locations (tubes 4 and 9 in A; tubes 1, 4, 6, and 8 in B). We neglect the precipitation at the initial electrolyte junction ($x = 0$). (2) Much fainter structures exist which contain considerably less precipitated material and are therefore not so easily recognizable (marked by open triangles).[18] (3) Additional structural features of still fainter contrast are striations in the spatial distribution of colloidal density, comparable to those mentioned in the previous section and in ref 5; they are not accounted for in the following. (4) The variation of the location and the total number of precipitation patterns of both qualitative categories (full and open triangles) from one tube to the next shows a distinct stochastic element. We seek to determine the probability of ring occurrence and the distribution in space of a band of a given number. There is some arbitrariness in identifying well-defined or faint bands and in assigning a number to a band in a specific tube. (Example: the only band in tube 7 of Figure 4B is counted as the second band and it is assumed that the first band has not formed as, for instance, in tube 6.) Nonetheless, a useful picture emerges.

2. Statistical Analysis. We proceed to a statistical analysis of the measured ring locations by plotting histograms for each of the eight systems of group B. For that purpose the number of tubes $M_j^{(n)}$ is counted for which the location of the nth ring falls into the jth space interval $x_j - \alpha/2 < x < x_j + \alpha/2$, where $x_j = (j + 1/2)\alpha$ ($j = 0, 1, \ldots$) and $\alpha = 0.2$ mm for series B-1,2 or $\alpha = 0.5$ mm for series B-3. The value of the sum

$$M_n = \sum_j M_j^{(n)} \tag{1}$$

is indicated for each histogram. Usually we have $M_n = M_{tot}$, meaning that the nth ring appeared in all prepared tubes of the specific system. However, there are faint rings which do not always form, and consequently $M_n < 0.5\, M_{tot}$ (histograms at $10 < x < 15$ mm in Figure 6B–D). In still other histograms we find $M_n > M_{tot}$, e.g., in Figures 5A ($n = 4$), 6D ($n = 2$), and 7, that is, for rings in regions of lowest concentration gradients (the last rings formed) and preferentially in systems with $\Delta \approx 0$. Under such conditions

TABLE III: Mean Values, $\bar{x}_n$, and Widths of the Distribution, δ_n, of Ring Locations for Series B-1 with Constant Δ = 13.6 mM[a]

$10^5\sigma$, M^3	$\bar{x}_1$, mm	δ_1^2	β_1, mm	$\bar{x}_2$, mm	δ_2^2	β_2, mm	$\bar{x}_3$, mm	δ_3^2	β_3, mm	$\bar{x}_4$, mm	δ_4^2	β_4, mm
2.1	1.0	0.34	0.33	2.9	1.93	0.79	7.6	5.1	1.28	17.0	-	-
1.3	1.3	0.87	0.53	6.6	1.36	0.66	14.1	4.4	1.19			
0.91	4.3	0.77	0.50	9.4	1.12	0.60	20.6	37.2	3.45			

[a] The values were computed by fitting a Gaussian distribution function (eq 2a) to the measured histograms (Figure 5). The quantity σ is the initial ion product and β_n is defined in eq 4.

TABLE IV: Mean Values, $\bar{x}_n$, and Widths of the Distribution, δ_n, of Ring Locations for Series B-2 with Constant $\sigma = 1.8 \times 10^{-5}$ M^3[a]

Δ, mM	$\bar{x}_1$, mm	δ_1^2	β_1, mm	$\bar{x}_2$, mm	δ_2^2	β_2, mm
10.8	4.2	1.56	0.71	20.5	9.4	1.74
2.4	6.9	1.43	0.68	17.7	25.8	2.87
0.9	6.7	2.35	0.87	19.1	29.6	3.08
0	4.9	6.20	1.41	21.9		

[a] Figure 6.

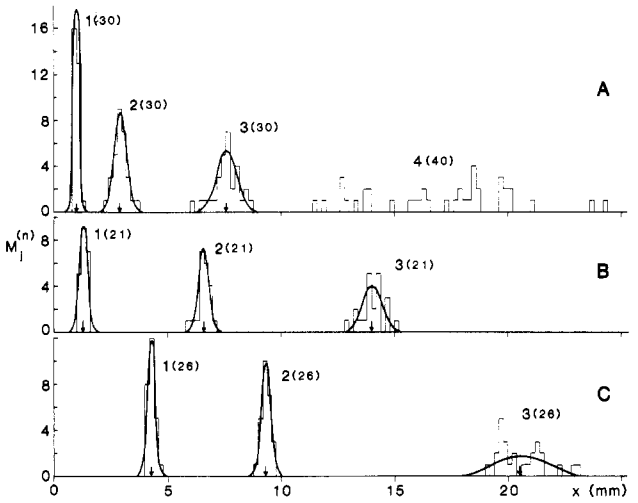

Figure 5. Histograms of the ring locations for $0 < x < 25$ mm in the tubes of series B-1 with Δ = 13.6 mM fixed: (A) $\sigma = 2.1 \times 10^{-5}$ M^3, (B) $\sigma = 1.3 \times 10^{-5}$ M^3, (C) $\sigma = 0.91 \times 10^{-5}$ M^3, see eq (1). The histograms are labeled with the respective ring number n. The numbers M_n (eq 1) for each ring appear in parentheses. A Gaussian distribution function (eq 2) is fitted to each ring histogram except for n = 4 in graph A. Mean values $\bar{x}_n$ for the ring locations are marked by arrows.

there form two rings with relatively narrow spacing. Since these rings fall into a small space interval, they contribute to one common histogram and are therefore represented by the same ring number n.

We fit each histogram by a Gaussian distribution located at the average value of the ring location $\bar{x}_n$ with a width δ_n

$$G^{(n)}(\Delta x_n) = M_{max}^{(n)} \exp[-(\Delta x_n)^2/(2\delta_n^2)] \quad (2a)$$

where

$$\Delta x_n = (x - \bar{x}_n)/\alpha \quad (2b)$$

$$\bar{x}_n = \frac{\sum_j M_j^{(n)} x_j}{M_n} \quad (2b)$$

$$\delta_n = \frac{1}{(2\pi)^{1/2}} \frac{M_n}{M_{max}^{(n)}} \quad (2c)$$

The width of the distributions δ_n is determined from

$$\sum_j [G^{(n)}(\Delta x_{nj}) - M_j^{(n)}]^2 = \min \quad (3)$$

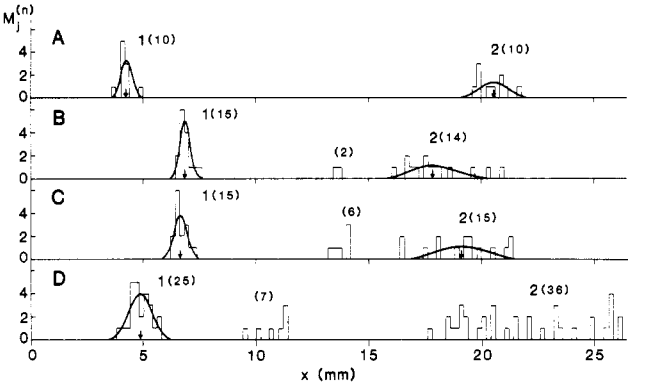

Figure 6. Histograms of the ring locations for $0 < x < 27$ mm in the tubes of series B-2 with $\sigma = 1.8 \times 10^{-5}$ M^3 fixed: (A) Δ = 108 mM, (B) Δ = 2.4 mM, (C) Δ = 0.9 mM, (D) Δ = 0, see eq 1. The histograms are labeled with the respective ring number n. (No number is assigned to those rings which appear in less than 50% of all tubes). The numbers M_n (eq 1 for each ring appear in parentheses. A Gaussian distribution function (eq 2 is fitted to each histogram except for n = 2 in graph D. Mean values $\bar{x}_n$ for the ring locations are marked by arrows.

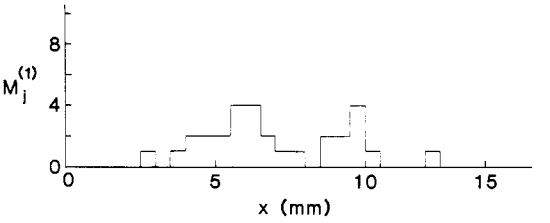

Figure 7. Histogram of the ring locations for $0 < x < 15$ mm in the tubes of series B-3 with $\sigma = 1.4 \times 10^{-5}$ M^3 and Δ = 0. The value of M_n (eq 1) is 30.

with

$$\Delta x_{nj} = (x_j - \bar{x}_n)/\alpha$$

$M_{max}^{(n)}$ is derived from eq 2c. The corresponding best fits are plotted for all but those histograms of Figures 5–7 for which it is immediately clear that a single-peaked Gaussian-type distribution function is not appropriate. The calculated values of $\bar{x}_n$ and δ_n for series B-1 and B-2 are listed in Tables III and IV, respectively. We include values of the quantity

$$\beta_n = (2)(2^{1/2})\alpha\delta_n \quad (4)$$

which measures the width of the distribution function at $(1/e)M_{max}^{(n)}$.

3. Discussion. As the ring number n and the average location x_n increase in each specific Liesegang system, so does the stochastic element in x_n. This increase of the width of histograms (or of β_n) in regions where the concentration gradients are low (x large) is best illustrated in Figure 5A with n = 1, ..., 4. As σ is lowered at fixed Δ (Figure 5A–C, Table III), for each n the locations x_n are clearly shifted to larger values (with a change of 1 in the total number of rings) but variations in β_n remain small, except for n = 3 in Figure 5C where σ is close to the value below which no structure is observed.[5] A decrease in Δ

at constant σ, on the other hand, always results in a pronounced broadening of the ring distributions ($n = 1, 2$ in Figure 6A–D and Table IV), while the dependence of $\bar{x}_n$ on Δ is less significant and nonmonotonic.[5]

The histograms are fairly well represented by a Gaussian distribution function except when $\bar{x}_n$ is large or $W \approx 0$; in those cases the probability of ring occurrence is almost evenly distributed in a broad space interval.

In several broad histograms two weakly pronounced maxima can be distinguished, e.g., in Figure 7 at $x = 6$ and 9.5 mm, and for $n = 3$ in Figure 5C at $x = 19.5$ and 21.5 mm. In systems with low Δ or σ there exist broad zones of colloidal material prior to ring occurrence and the final ring locations frequently coincide with one of the edges of such zones (see section III.B in ref 5). There is visual evidence for broad zones of colloid in the tubes investigated here, and it would be interesting to obtain more measurements on the correlation between the spatial distribution of colloid and the probability distribution of ring locations.

Rings with low probability of occurrence ($M_n < 0.5M_{tot}$) are found in systems with Δ close to zero; they disappear ($M_n \to 0$) when Δ is increased, as shown by the histograms without ring number in Figure 6. The situation $M_n > M_{tot}$ arises preferentially in those histograms where $\bar{x}_n$ is large and the stochastic element in x_n is particularly pronounced.

C. Pattern Formation without Imposed Gradients of Concentration. The formation of spatially nonuniform distributions of precipitate in initially uniform colloids of PbI_2 has been reported previously.[6,7,9,21] In further studies of PbI_2 systems prepared under gradient-free conditions (group C of experiments, see section II.A) we found different varieties of structure. We report three examples which can be roughly characterized as a two-dimensional network (Figure 8A), a wavelike structure (Figure 8B), and a speckled pattern (Figure 8C). Concentration specifications are given in the caption. The wavelike structures are reminiscent of Liesegang patterns. The preparation procedure was the same for all examples and we do not know the experimental conditions which lead to one type of structure or another. It appears that not only the choice of initial concentrations but slight differences in the preparation history of the samples are of substantial influence. The patterns are stochastic rather than deterministic and are characterized by length scales which, in general, range from 0.5 to 10 mm.

The dense regions of PbI_2 of gradient-free structures consist mostly of independent colloidal particles, the size of which strongly depends on the initial supersaturation of the salt. A certain but small degree of coagulation occurs. The dense regions are separated by spaces essentially devoid of such particles.[9]

IV. Conclusions

In this and prior articles[4–6,8,9] we showed that the formation of macroscopic structure in precipitation is governed by postnucleation processes in systems both with and without concentration gradients. In the presence of large gradients, which is the condition for the standard Liesegang experiment, the location of the rings is deterministic. As the gradients are decreased, the location of rings becomes stochastic (random). In the limit of no concentration gradients various types of macroscopic random structures are formed. In each case, with or without imposed gradients, there is a lower limit to the initial ion product below which no structure formation occurs. The experiments presented here were chosen to show the continuous progression of structure formation from high to zero initial concentration gradients, and thus lead to the suggestion that the origin of pattern formation is the same in all cases.

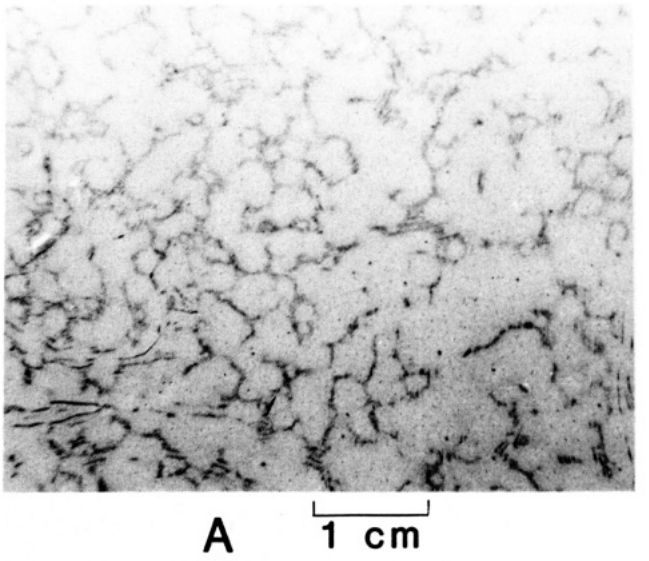

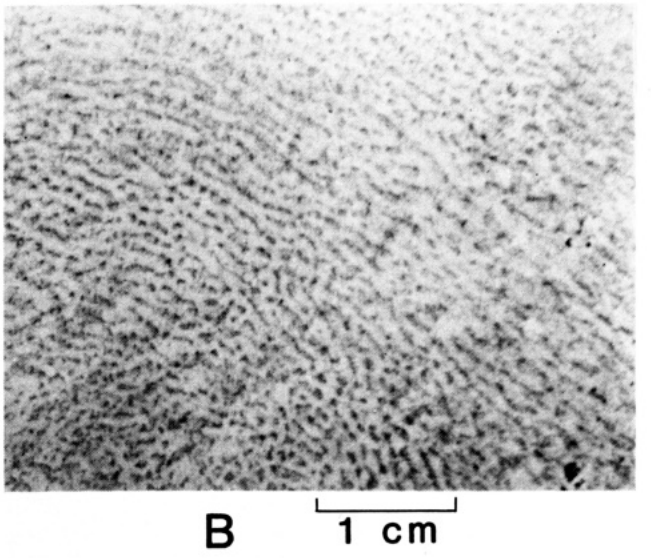

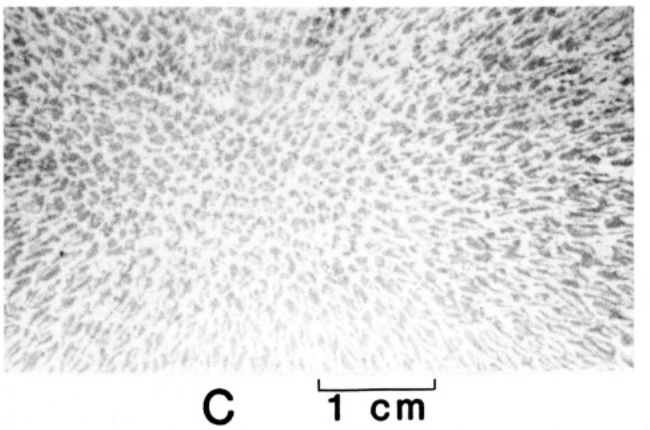

Figure 8. Three types of precipitation patterns of PbI_2 in agar gel without imposed gradients of concentration. The systems were prepared in Petri dishes of diameter 90 mm with a layer thickness of 1.5 mm. The patterns evolved at 22 °C. The concentrations of PbI_2 and agar gel were respectively as follows: (A) 5.2 mM, 1%; (B) 6.1 mM, 0.2%; (C) 5.4 mM, 0.5%. The length scales are approximately 6 (A), 1.2 (B), and 1.5 (C) mm.

(21) J. Ross, *Ber. Bunsenges. Phys. Chem.*, **80**, 1112 (1976).

The Ostwald-Wagner-Prager[11-13] theory of Liesegang ring formation postulates that nucleation is discontinuous in space and determines the ring locations. This is contrary to our findings. Furthermore, the theory does not apply to the case of no imposed spatial gradients. A theory of structure formation has been proposed which is based on a chemical instability[6,7,14,15] due to autocatalytic colloidal growth, after nucleation, coupled with diffusion. The theory applies to cases with, and without, initial concentration gradients. The basic assumptions of the theory need substantial further development so that they can be tested against the many details of the experiments reported.

Acknowledgment. This work was supported in part by the National Science Foundation and by the Air Force Office of Scientific Research.

Registry No. PbI_2, 10101-63-0.

Temperature Dependence of the Nonradiative Relaxation Process of the Lowest Excited Singlet States of Meso-Substituted Bromoanthracenes

Masanao Tanaka, Ikuzo Tanaka,

Department of Chemistry, Tokyo Institute of Technology, Ohokayama, Meguro, Tokyo 152, Japan

Shigeyoshi Tai, Kumao Hamanoue,*

Department of Chemistry, Kyoto Institute of Technology, Matsugasaki, Sakyo, Kyoto 606, Japan

Minoru Sumitani, and Keitaro Yoshihara

Institute for Molecular Science, Myodaiji, Okazaki 444, Japan *(Received: March 1, 1982; In Final Form: October 4, 1982)*

Direct measurements of the temperature dependence of the fluorescence lifetimes of 9-bromoanthracene (BA) and 9,10-dibromoanthracene (DBA) have allowed the determination of the rate constant for intersystem crossing (isc) in the form $k_{isc} = A_{isc} \exp(-\Delta E/kT)$. This isc is attributed to that from the lowest excited singlet state S_1 to an adjacent higher excited triplet state T_n. The values of ΔE, i.e., 600–710 cm^{-1} for BA and 1100 cm^{-1} for DBA, are about 300 cm^{-1} larger than those deduced from the $T_n \rightarrow T_1$ fluorescence (TTF) measurement by Gillispie and Lim (*Chem. Phys. Lett.*, **63**, 355 (1979)). The values of the S_1 decay constants consistent with those of the buildup times for triplet–triplet absorptions lead us to the suggestion that the T_n lifetimes are tens of picoseconds, and this estimate gives good agreement between calculated and experimental Φ_{TTF} of DBA.

Introduction

Recently, the study of the nonradiative process of the fluorescing state in anthracene derivatives has received considerable attention from both experimental and theoretical points of view.[1] Since the rate of intersystem crossing (isc) is proportional to the vibrational overlap factor whose magnitude increases rapidly with decreasing energy gap between the two interacting states,[2] the large S_1–T_1 separation of anthracenes makes the direct isc to T_1 of minute importance because of the extremely unfavorable vibrational overlap factor for such a process. As a result, the number and the order of the higher triplet state(s) lying near or very slightly above the lowest excited singlet state may be expected to be important for isc.

The existence of such higher triplet states has been supported by the following experimental results: (1) Rather long buildup times of the triplet–triplet absorption (72–86 ps) for nonfluorescent nitroanthracenes (9-nitro-, 9-benzoyl-10-nitro-, and 9-cyano-10-nitroanthracene) lead us to the conclusion that the observed buildup times do not reflect the lifetimes of the singlet states but might represent the rates of nonradiative process in the triplet manifold, and that the indirect isc $S_1(\pi\pi^*) \rightarrow T_n(n\pi^*) \rightarrow T_1(\pi\pi^*)$ is the most important process to populate T_1.[3] (2) The $T_2(^3B_{1g})$ state is found to lie below S_1 by 600, 600, and 900 cm^{-1} for anthracene,[4,5] 2-methylanthracene,[5] and 1,5-

(1) J. B. Birks, "Photophysics of Aromatic Molecules", Wiley-Interscience, New York, 1970, Chapters 4 and 5.
(2) G. W. Robinson and R. P. Frosh, *J. Chem. Phys.*, **37**, 1962 (1962); **38**, 1187 (1963).
(3) K. Hamanoue, S. Hirayama, T. Nakayama, and H. Teranishi, *J. Phys. Chem.*, **84**, 2074 (1980).
(4) R. E. Kellogg, *J. Chem. Phys.*, **44**, 411 (1966).
(5) Y. H. Meyer, R. Astier, and J. M. Leclercq, *J. Chem. Phys.*, **56**, 801 (1972).

0022-3654/83/2087-0813$01.50/0